AD NUMBER
AD823715
LIMITATION CHANGES

TO:

Approved for public release; distribution is unlimited.
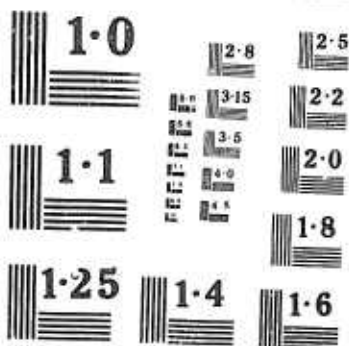
FROM:

Distribution authorized to U.S. Gov't. agencies and their contractors; Administrative/Operational Use; OCT 1967. Other requests shall be referred to Office of Naval Research, Washington, DC 20360.

AUTHORITY

onr notice, 27 jul 1971

AD 823715

NATIONAL BUREAU OF STANDARDS
MICROCOPY RESOLUTION TEST CHART

SPECTRAL PROPERTIES OF PASSIVELY Q-SPOILED LASERS

SemiAnnual Technical Summary Report

Contract Nonr-5150 (00)
ARPA Order Number 306
Project Code Number 015-710

A 32-Month Contract
From 1 October 1965 through 30 June 1968

30 October 1967

PROJECT SCIENTIST

B. H. Soffer

PROGRAM CONTRIBUTORS

R. C. Pastor
H. Kimura
J. Linn
B. McFarland

KORAD CORPORATION
A Subsidiary of Union Caride Corporation
2520 Colorado Avenue
Santa Monica, California
213/393-6737

TABLE OF CONTENTS

* * *

APPENDIX:

"Reversible and Irreversible Decay of Polymethine
Dye Solutions", R. C. Pastor, H. Kimura, and
B. H. Soffer.

LIST OF FIGURES

ABSTRACT

Two new blue-violet organic dye lasers are described. Another blue-violet system, a frequency doubled near-infrared organic dye laser, is also described. The results of incorporating a bleachable absorber into the organic dye laser cavity are discussed. Further developments in the study of photobleaching of dyes used for Q-spoiling the Nd laser are reported. A preprint of an article submitted for publication, based on work supported by this contract, is reproduced as an Appendix.

FOREWORD

This report was prepared jointly by the Optical Physics and Chemical Physics Divisions of Korad Corporation, Santa Monica, California, under Contract Nonr-5150(00) entitled "Spectral Properties of Passively Q-Spoiled Lasers". The study was conducted under the project leadership of B. H. Soffer with R. C. Pastor, H. Kimura, J. Linn, and B. B. McFarland participating.

Section 1

INTRODUCTION

The objective of this program is an experimental research
study of the spectral properties of passively Q-spoiled lasers
and the properties of the recently developed organic dye lasers.
The study is directed toward a further understanding of the
spectral and physical behavior of laser and Q-spoiling materials.

In the previous SemiAnnual Technical Summary Report we
reported work on the visible stimulated emission from organic
dyes and the demonstration of a continuously-tunable narrow-
band organic dye laser. During this report period we have in-
vestigated two methods of extending these ideas to operation
in the blue-violet spectral region. Two new organic dye laser
materials operating in this region are reported upon. These
results are compared with the results of frequency doubling a
near infrared organic dye laser. The effects of incorporating
bleachable absorbers into the organic dye laser cavity are
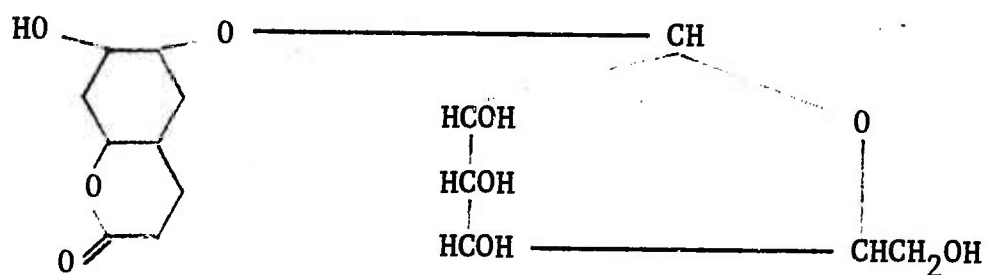described.

Section 2

TECHNICAL DISCUSSION

A. Stimulated Emission in Organic Dyes

(1) New Dye Laser Materials

Two new, blue-violet emitting organic dye laser materials were found in this period: Esculin and Acridone. The structural chemical formulas of these species are shown in Figure 1. The room temperature absorption and fluorescence spectra of these molecules in methanol solutions are displayed in Figure 2. Both species exhibit the typical mirror symmetry of absorption and fluorescence characteristic of organic compounds, but it can be seen that the vibrational and other structural features evident in the spectrum of Acridone (upper trace) are mitigated in the diffuse and broad spectra of Esculin. This may be caused by the sugar-like part of the Esculin molecule (cf. Figure 1) whose many possible steric forms may be responsible for an inhomogeneously broadened spectrum. Furthermore, this sugary part of the molecule imparts a small optical rotary power whose effects upon the generation of stimulated emission are of interest although no effects directly connectable with the rotation have, as yet, been discerned. Related molecules, less the sugar-like part, are being obtained to help resolve these points. The laser output when pumped with the second harmonic output of a giant pulse ruby laser (347 mµ), was found to be two times greater for the Acridone than for the Esculin solution (at optimum concentrations). The broad output of wavelengths for both dyes was centered in the neighborhood of 434 mµ. It should be noted (cf. Figure 2) that self-absorption in this region is more significant for Esculin

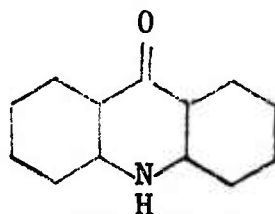The structural formulas of

Esculin

and

Acridone.

Figure 1

Upper trace: Room temperature absorption and fluorescence of Acridone in methyl alcohol.

Lower trace: Room temperature absorption and fluorescence of Esculin in methyl alcohol.
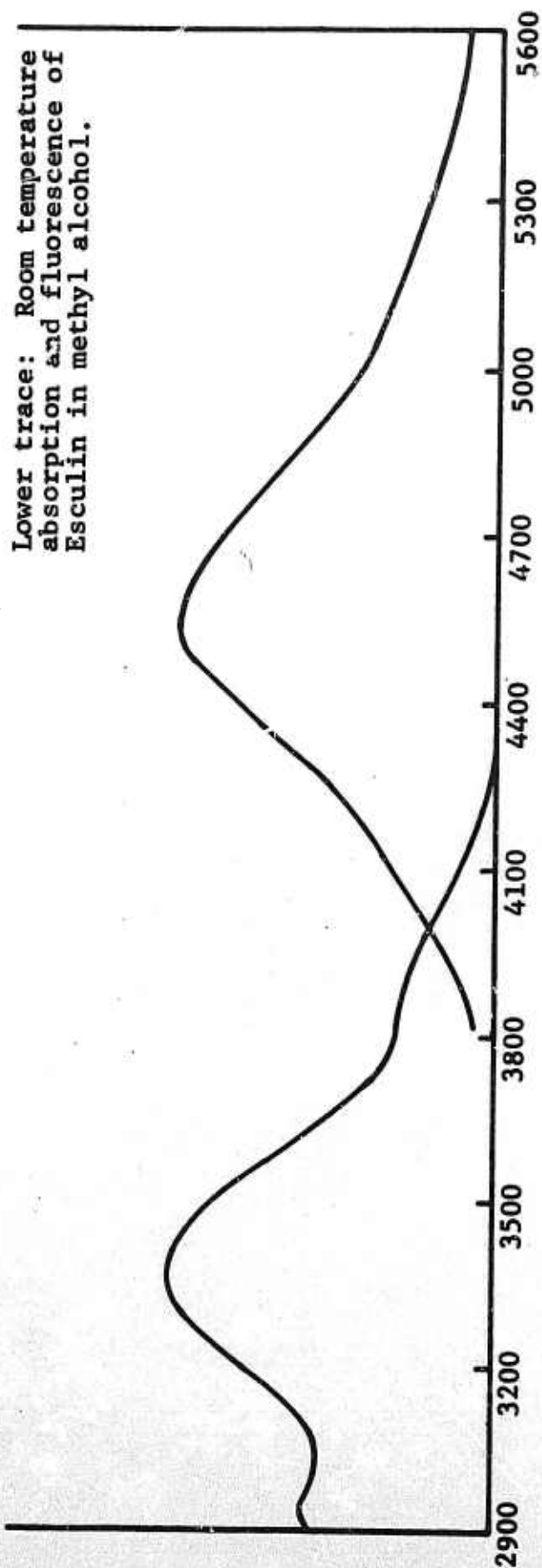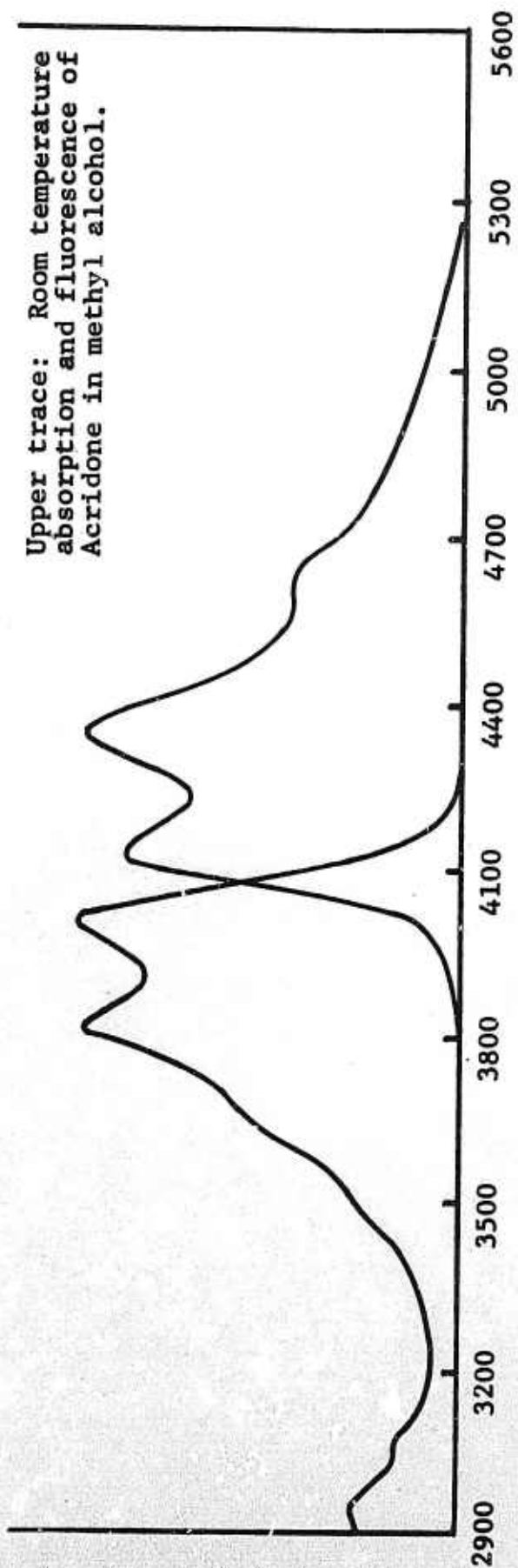
Figure 2

(lower trace) than Acridone (upper trace). The Acridone laser
at outputs of 1.5 megawatts had a power efficiency of 0.9%
defined as output divided by ruby fundamental input. The ADP
doubling crystal with an effective area of 0.6 cm^2 worked at
5% efficiency.

It is interesting to note that the added presence of
50 Mw/cm^2 ruby emission (694 mμ) in the pumping light tends to
inhibit the lasing of Acridone but not of Esculin. The output
was reduced to 0.5 Mw and the efficiency to 0.25% (including
corrections for filter factors). As the ground state of Acridone
does not absorb ruby light, one may ignore the possibility of
thermal degradation of the optical quality of the Acridone laser
and conclude that the effect is due to an excited state absorption
from the upper lasing level.

(2) Frequency Doubling the Organic Dye Laser

Experiments were performed with an ADP frequency doubling
crystal in the organic dye laser cavity. Pumping a solution of
the dye 3,3' diethyl-thia-tricarbocyanine iodide was effected
with ruby fundamental laser radiation. The broad 190 $\overset{o}{A}$ wide
spectral emission of the fundamental near 0.8μ transforms into
narrowed 20 $\overset{o}{A}$ wide second harmonic output. A calculation of phase
matching angles for efficient second harmonic generation vs.
wavelength for ADP, using published index values shows the ob-
served 20 $\overset{o}{A}$ spectral width to be consistent with a 4×10^{-3}
radian beam angle. At a given orientation only a fraction of
the available wavelengths in the fundamental are efficiently phase
matched for frequency doubling. The wavelength of emission can
be tuned by rotating the doubler crystal but the output power
falls rapidly following the square of the fundamental power vari-
ation with wavelength. A diffraction grating was used, as
described earlier, as a cavity reflector to efficiently condense

the output into a single narrow 2 $\overset{\circ}{A}$ line using a 1200 ℓ/mm grating. To span the whole useful range with good efficiency the doubler crystal, as well as the grating, must be rotated. The lasing efficiency of Acridone, using a fixed ruby fundamental power, was compared to that of the 3,3' diethyl-thia-tricarbocyanine iodide operating with the frequency doubler in the cavity. Acridone with $\eta = 0.9\%$ had twice the power efficiency. However, the reflectivity of the cavity mirrors was not optimized at both fundamental and harmonic frequencies to capitalize on possible regenerative effects of the doubled light.

A highly structured channeled spectrum was sometimes observed with this system (less the grating) but with poor reproducibility. These channelings have also been observed without the incorporation of a doubler crystal. As they have not been observed in a system operating with a specially constructed cell having Brewster windows on all surfaces, internal and external, we believe they must have occurred by accidental Fabry-Perot type resonance in the cavity.

(3) Incorporation of Absorbers into the Organic Dye Laser Cavity

Putting separate solutions of Ethyl-Red, a bleachable absorber, whose peak absorption matches the emission of Rhodamine 6G (cf. Figure 3) into the cavity of a Rhodamine 6G dye laser effected some 300 $\overset{\circ}{A}$ of tuning of the output as well as a certain amount of variation in spectral width as the concentration of the absorber was changed. These results are displayed graphically in Figure 4 by the horizontal bars whose vertical position and lengths indicate the wavelength and spectral bandwidth of emission for the concentrations indicated on the abscissa. These effects may be understood by considering the absorption curve of Ethyl-Red in conjunction with the spectral gain profile of
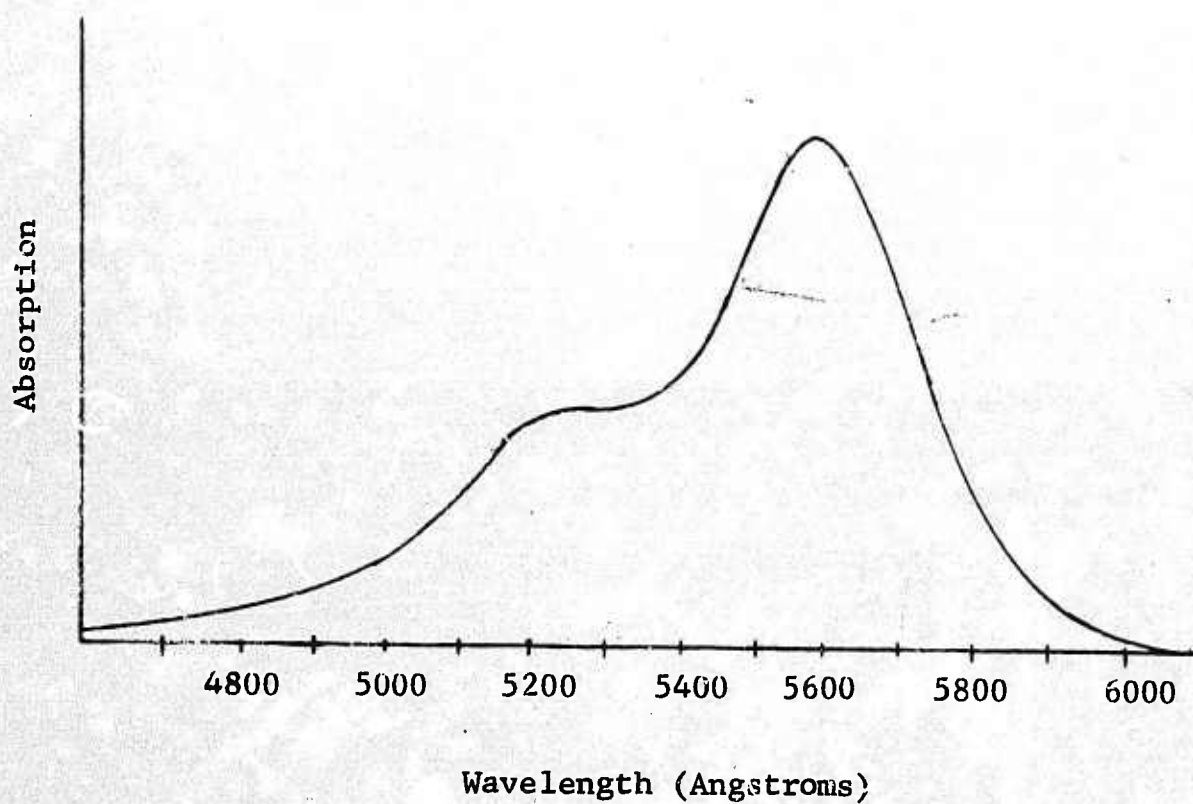
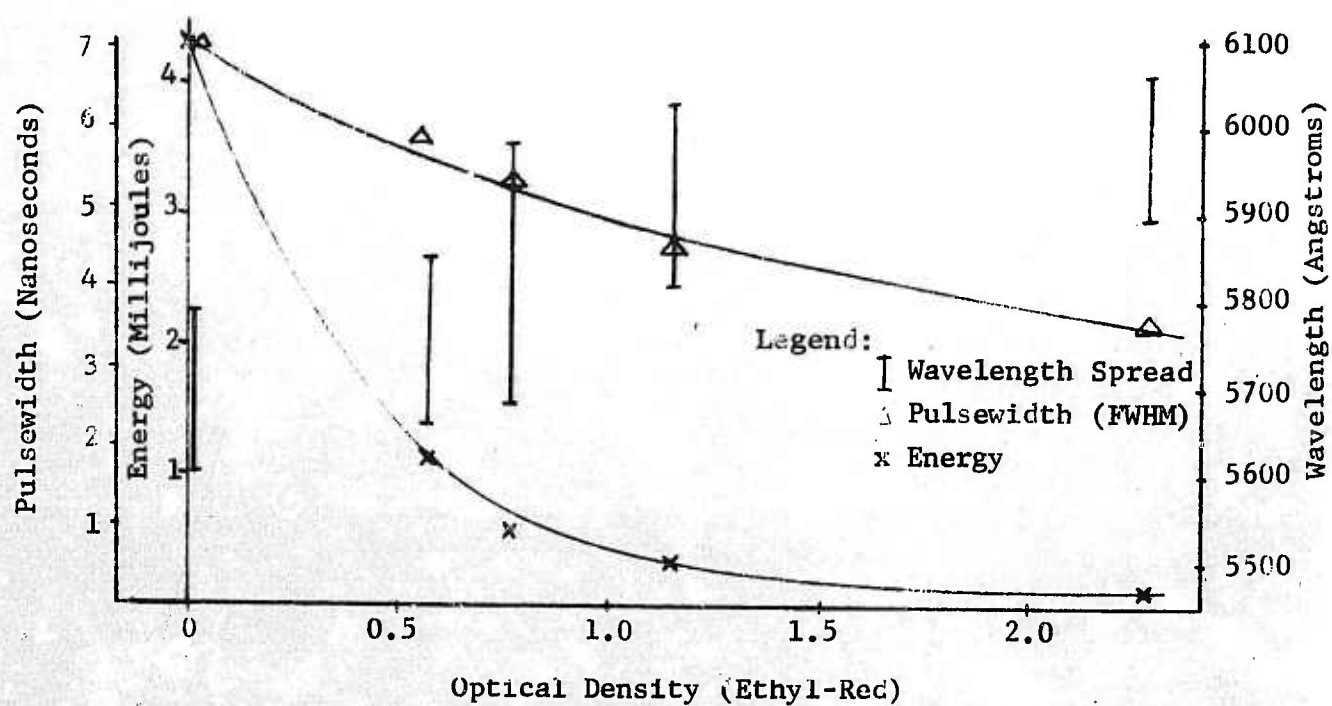Figure 3

Room Temperature Absorption of Ethyl-Red in Ethanol

Figure 4

Variation of pulsewidth, energy, and wavelength of a Rhodamine 6G laser as function of ethyl-red peak optical density.

the Rohodamine 6G to obtain a new net gain function. As also
shown in Figure 4, the pulsewidth of the output was narrowed
by as much as a factor of two with increasing concentration
of absorber, but the energy content of the pulses diminish
more rapidly so no net power gain was realized by this technique.
This latter result was also obtained when, in addition, a grating
was employed in the cavity to constrain the output to a specific
wavelength. Similar results were obtained with other bleachable
absorbers such as, for example, some of the common colored glass
filters.

B. Reversible and Irreversible Bleaching of Dyes for Passive Q-Spoiling

Selective photobleaching of the fundamental 1μ absorption
band, under low intensity irradiation, was studied in solutions
of KQS* (pentacarbocyanine dye). Three prominent absorptions,
0.52μ, 0.46μ and 0.38μ (molar extinction coefficient: 10^4), were
examined. Bleaching was effected in quinoline and chlorobenzene
at 0.38μ with 8×10^{-4} watts cm^{-2} incident, and at 0.46μ with
6×10^{-3} watts cm^{-2} incident, but not at 0.52μ with 8×10^{-3}
watts cm^{-2} incident. The decay with respect to the fundamental
was zero order.

It appears that a certain amount of absorption by the solvent
is necessary for bleaching. Bleaching at 0.38μ where solvent
absorption is more intense, is at least one order of magnitude
more efficient than at 0.46μ. Also, bleaching is more efficient
in quinoline than in chlorobenzene, the latter solvent being
weaker-absorbing. Reversible and irreversible bleaching is,
therefore, a behavior of the dye-solvent complex with excited
states of both components involved in the process. In the case
of methanol, which solvates tightly to the polar dye and is
transparent to the region of irradiation, neither KQS nor krypto-
cyanine exhibits reversible or irreversible bleaching.

---

*Korad Q-Spoiling Solution.

A final analysis of experimental errors, and some checks for self consistency among the several experimental methods used to derive the various previously reported results, were performed. A paper was written incorporating all the results previously reported, and submitted for approval for publication. A preprint is attached as an Appendix to this report.

Section 3

PLANS FOR NEXT PERIOD

A study will be made of molecules related to Esculin to determine the influence of the sugar-like part on the spectral and lasing behavior of Esculin. A third Nd glass laser rod is being fabricated with Brewster windows in order that work may begin on experiments on the mode locking of the organic dye laser systems.

APPENDIX

Reversible and Irreversible Decay
of Polymethine Dye Solutions

REVERSIBLE AND IRREVERSIBLE DECAY OF POLYMETHINE DYE SOLUTIONS*

R. C. Pastor, H. Kimura, and B. H. Soffer

Korad Corporation
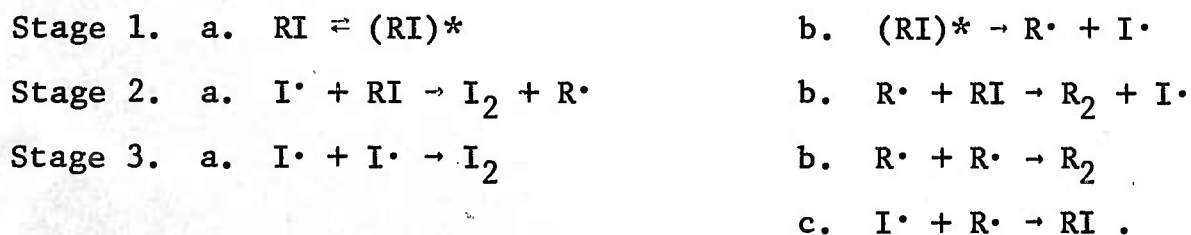A Subsidiary of Union Carbide Corporation
Santa Monica, California

A B S T R A C T

A reaction scheme is presented to characterize the stability of solutions of polymethine dyes with respect to other chemical species, temperature, and radiation. The observed equilibrium properties as well as the kinetic and steady-state parameters favor a model on a low-lying triplet state.

I. INTRODUCTION

Three polymethine dyes used in passive Q-spoiling of lasers are: kryptocyanine,[1] KQS,[2] and EQS.[3] All three solutions bleach (decay) reversibly and irreversibly to varying degrees under repetitive Q-spoiling. These shortcomings prompted a study of the effects of chemical species in the environment, temperature, and radiation. In the homogeneous-phase decay of dilute solutions, the reaction scheme which plays the central theme has three stages. The dye in the iodide form and the molecule in the ground singlet state is represented by RI.

Stage 1. a. $RI \rightleftharpoons (RI)*$ b. $(RI)* \rightarrow R\cdot + I\cdot$

Stage 2. a. $I\cdot + RI \rightarrow I_2 + R\cdot$ b. $R\cdot + RI \rightarrow R_2 + I\cdot$

Stage 3. a. $I\cdot + I\cdot \rightarrow I_2$ b. $R\cdot + R\cdot \rightarrow R_2$

       c. $I\cdot + R\cdot \rightarrow RI$.

The nature of the intermediate, $(RI)*$, will be taken up in Section III. Stages 2 and 3 are conventional in free-radical reactions. The latter is a throttle to the former. These do not involve large activation energies, i.e., stage 1 provides the limiting rate. Stage 1.a. depicts reversible bleaching.[4] The rest is irreversible, an approximation valid for extremely dilute solutions.

II. MATERIALS AND APPARATUS

Kryptocyanine and EQS were obtained from Eastman Organic Chemicals. KQS was synthesized in the laboratory.[2] The solvents were methanol, quinoline, and chlorobenzene; spectrophotometric-grade reagents of J. T. Baker Chemical Co. The concentrations were 10^{-5} M (molar).

Optical density was measured in a 1-cm cell with a Beckman DK-1A, provided with a temperature-regulated cell holder. Con-

trol samples established the warm-up half-life for the cell assembly. A xenon-arc lamp, in conjunction with a 500-mm focal length grating monochromator, was used for irradiation in the visible and the near visible. More intensive irradiation at 1.06μ was carried out with a Nd-YAG laser (12 watts cw); for the near uv, a conventional high-pressure mercury-arc lamp was focussed into the cell. In KQS or EQS solutions, the 1μ-absorption was probed normal to the beam with a PbS-detector. Energy flux at the site of irradiation was measured with an Eppley thermopile.

III. RESULTS AND DISCUSSION

A. Effect of Chemicals

Reversible bleaching by a change in pH is neither of interest nor pertinent to the working model. The irreversible bleaching considered is that caused by species in the environment at constant temperature in the dark. Stage 3.a. provides a basis for forced irreversible bleaching. At room temperature ($27^{\circ}C$), the reverse direction has a half-life 10^{12} sec and the equilibrium constant for dissociation is 10^{-22} moles per liter.[5] As expected (stage 2), complete decomposition in the dark proceeds rapidly, limited by diffusion, when equivolumes of $10^{-5}M$ I_2 and KQS in methanol are mixed.[6] Thus, 10^8 RI per iodine atom is consumed in $\ll 1$ sec.

A vacuum manifold was employed to prepare KQS-quinoline in optical cells, to study the effect of oxygen. A known amount of dye as KQS-methanol was introduced into the cell. The solvent was removed by pumping. A known volume of quinoline, dried and refluxed in a column containing Mg turnings, was distilled into the cell. One cell was sealed under 0.42 mm and the other under 1.00 mm pressure of oxygen. All operations were carried out in the dark. Over a 300-hr interval, the decay of the fundamental (1μ-band) at room temperature was first order, 0.41% hr^{-1} for the 0.42 mm case and 0.44% hr^{-1} for the other, i.e., $\tau = 163$ hr. The decay was not limited by the passage of oxygen across the gas-liquid interface. It is argued later (cf. III.B.) that (RI)* was

the reactive species. A dark-reaction with oxygen is shown by all the solutions examined.

Stage 1 is dependent on the solvent. In the absence of oxygen, room-temperature stability of KQS solutions in the dark, in decreasing order, is methanol > chlorobenzene > quinoline >> α-chloronaphthalene. The stability ranges from no decomposition in methanol after a two-year storage to a half-life of two days in α-chloronaphthalene. In the presence of oxygen (air), under the same conditions, the respective half-lives are shorter, 3.7 hr in methanol, 120 hr in chlorobenzene, and 3-6 hr in quinoline.

The variable behavior in quinoline is caused by moisture which shows a catalytic influence. The following room-temperature response in the dark of KQS-quinoline (first-order decay) is typical: dry oxygen bubbled through, τ = 4 hr; followed by dry nitrogen, after flushing out the previous gas, no decomposition in 15 hrs; wet nitrogen, τ = 30 hr, presumably due to a small background of oxygen; wet oxygen, τ = 0.13 hr. In kryptocyanine-water, the action of oxygen is striking. Material precipitates out. The deoxygenated solution is stable for indefinite periods.

B. Effect of Temperature

From Section I, the working model is,

$$\text{Model I:} \quad RI \underset{k_r}{\overset{k_f}{\rightleftharpoons}} (RI)* \overset{k_i}{\longrightarrow} \quad \cdots .$$
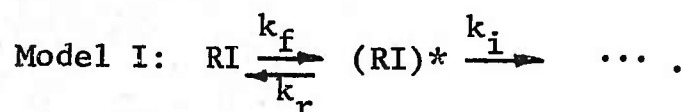
The k_i-path, as well as the reaction paths of the free radicals (stage 1), depend on the impurities (cf. III.A.), temperature, and radiation. In the study of thermal bleaching, spectrophotometric-grade materials were employed. Distillation of solvent and preparation of solutions were performed in vacuum (cf. III.A.). The optical cells were sealed. All operations

were carried out in the dark, except for the probe at the fundamental.

Completely reversible bleaching means

$$k_i = 0 \; ; \tag{1}$$

and

$$y_{rev} = \frac{1}{1 + K} \left[1 + Ke^{-k_r(1 + K)t} \right] \; . \tag{2}$$

The concentration of RI is normalized; $y_{rev} = 1$ at $t = 0$, and

$$K = k_f/k_r \; . \tag{3}$$

The reversible-irreversible case where

$$k_f \gg k_i \; , \tag{4}$$

is given by

$$y = \left[\frac{k_f - \frac{\beta}{\alpha}}{\alpha - \frac{\beta}{\alpha}} \right] e^{-\alpha t} + \left[\frac{\alpha - k_f}{\alpha - \frac{\beta}{\alpha}} \right] e^{-\frac{\beta}{\alpha} t} \; , \tag{5}$$

where

$$\alpha = k_f + k_r + k_i \tag{6}$$

and

$$\beta = k_f k_i \tag{7}$$

The model explains thermal bleaching of KQS-quinoline in the measured range 40°-180°C, and EQS-chlorobenzene from 35° to 124°C. Unlike photo bleaching (cf. III.C.), only a general reduction in the absorption spectrum resulted from heating. The constants derived from curve analysis are plotted in Fig. 1. The dependence summarized in Table I was calculated by the method of least squares. The assumed inequality (4) is borne out. Due to the low value of k_i, stage 1.b. throttled stage 2, which otherwise, would have provided another decay path to RI.

The ratio of RI to solvent, 10^{-7}, is readily exceeded by that of impurities in reagent-grade materials. The rate constants were derived from total bleaching. A pertinent test of the model and reproducibility of the preparation is a prediction of the reversible fraction. If the solution is held at a temperature over a time interval $\Delta t \gg (k_f^{-1}, k_r^{-1})$, the fraction decomposed equals $K k_i \Delta t$. Table 2 compares the reversible fraction of two solutions. Fig. 2 shows prediction vs. observation for the recovery of EQS-chlorobenzene after a 20-hr exposure.

Within the accuracy of the experiment, the enthalpy change for reversible bleaching and the energy barrier to irreversible bleaching is the same in the two solutions (cf. Table I). From equation (3), no activation is involved in k_r(EQS) which has τ_r (EQS) = 0.3 min. A small barrier, 600 cal mole^{-1}, exists in KQS-quinoline where, τ_r (KQS) = 3 min at 27°C.

An interpretation of the nature of (RI)* is relevant. This intermediate does not appear to be a geometric isomer, there being only a general reduction in absorption. The frequency factor of k_f and k_r is very low. The energy barrier for recovery is marginal. (RI)* is most likely a low triplet, an "electronic isomer".[7] Since $k_f^{-1} \ll 163$ hr (cf. III.A.), a reaction between triplets would explain the dark-reaction with oxygen. And similarly with solvent stability where the sequence in

III.A. corresponds to decreasing solvent triplet-energy for the rarefied state. Since only RI was measured, any mechanism first order with respect to (RI)* would be in harmony with the results. However, in view of the reproducibility of the preparations and the low value of k_i, we believe that the path measured is intrinsic to the solute-solvent pair.

C. Effect of Radiation

Two main absorptions in the near visible characterize the solutions (cf. Fig. 3 below). In a given dye the position and absorption strength depend on the solvent.[8] The fundamental, one of the two main absorptions, has $\epsilon \approx 10^5$ liter mole^{-1} cm^{-1}. The two components of the fundamental are attributed to the cis and trans arrangements, the latter accounting for the lower-frequency absorption.[9] No observable bleaching resulted from low-intensity (10^{-2} watts) irradiation of KQS-quinoline at the fundamental.

More intensive irradiation of KQS-quinoline by a Nd-YAG laser (1.06μ) with energy inputs $\geq$ 50 joules into a 3 cm^3 solution, gave no response beyond a percent which is accounted for by thermal bleaching (cf. III.B.). Intersystem crossing from the first excited singlet, k_{2r}, is negligible compared to internal conversion, k_{21}, a feature pertinent to Q-spoiling. (Subscript 1 for the ground state, 2 for the first excited singlet and r for the first triplet.) Steady state between levels 1 and 2 is reached immediately, and since

$$k_{2r} \ll k_{21} , \tag{8}$$

the steady-state distribution is

$$\bar{n}_2 k_{21} \approx \bar{n}_1 k_{12} . \tag{9}$$

APPENDIX

The duration of irradiation, τ_R, is much less than k_{r1}^{-1} (corresponds to k_r in III.B.). The fraction bleached, f, is

$$\bar{n}_2 k_{2r} \, \tau_R = f \, \bar{n}_1 \, . \qquad (10)$$

The total number of photons absorbed, N, is given by

$$N = \bar{n}_1 k_{12} \, \tau_R \, V \qquad (11)$$

where V is the volume of the solution. It follows from equations (9), (10) and (11) that

$$k_{2r} \approx \frac{f \, \bar{n}_1 \, V}{N} k_{21} \, . \qquad (12)$$

From the results given above, $N \geq 3 \times 10^{20}$, $f < 0.1$, $V = 3 \text{ cm}^3$ and $\bar{n}_1 = 10^{15} \text{ cm}^{-3}$; therefore, $k_{2r}/k_{21} < 10^{-6}$, in agreement with inequality (8). Disregarding the population of the triplet level, the saturation behavior of the fundamental absorption in kryptocyanine-CH_3OH, EQS-chlorobenzene and KQS-quinoline yields an interconversion rate of $k_{21} = 10^{11} \text{ sec}^{-1}$. Hence, in KQS-quinoline the intersystem-crossing mean lifetime is $k_{2r}^{-1} > 10^{-5}$ sec.

The other absorption, $\varepsilon \approx 10^4$ liter mole^{-1} cm^{-1}, shows three components in KQS solutions, 0.52μ, 0.46μ and 0.38μ. Bleaching was effected in quinoline and chlorobenzene at 0.38μ with 8×10^{-4} watt incident and at 0.46μ with 6×10^{-3} watt incident, but not at 0.52μ with 8×10^{-3} watt incident. The decay with respect to the fundamental appeared to be zero order, relaxation to the ground state being dominant. Data on room-temperature irradiation of air-free solutions are collected in Table 3. The number of photons absorbed per molecule bleached is

$$\eta(\lambda) = \frac{I_o(\lambda) \, \zeta F \cdot \varepsilon(1\mu) \cdot \ell}{6.0 \cdot 10^{20} V |A|} \qquad (13)$$

where $I_o(\lambda)$ is the photon flux centered at λ, the irradiation wavelength. To calculate the fraction absorbed, F, a Lorentzian shape for the components in the absorption envelope and a triangular energy-distribution function from the monochromator were assumed. The geometric factor was $\zeta \approx 1$, the volume of the solution $V = 3.0\ cm^3$ and the cell thickness $\ell = 1.0\ cm$. The initial optical density, D_o, and the decline per unit time, A, during irradiation refer to the probe (fundamental) where $\epsilon(1\mu) = 1.2 \times 10^5$ liter mole^{-1} cm^{-1} in both solvents.

The absorption coefficient of the solvent, $\alpha(\lambda)$, shows that bleaching efficiency improves with solvent absorption. At 0.46μ where the solvent is weakly absorbing, η seems independent of the solvent. If true, linear extrapolation to $\alpha = 0$ at 0.38μ would yield an intrinsic η. The existence of an intrinsic η is contradicted by KQS-methanol. No bleaching was effected at an irradiation dose (0.37μ) one order of magnitude larger. Absorption and photo-bleaching are clearly characteristic of the dye-solvent complex. In the calculation of F, $\alpha(\lambda)$ was not subtracted from the absorption coefficient of the solution. The last two columns in Table 3 are taken up below.

Under low-intensity irradiation, bleaching rate was established at $\tau_R < 10^2$ min. With $\tau_R = 2.6 \times 10^3$ min at 0.46μ, 6×10^{-3} watt incident, the total bleaching of KQS-quinoline was 25%. The irreversible fraction was $> 90\%$. This was not unexpected when $k_i \tau_R \approx 1$ for the fastest k_i-path. The solvent stability sequence (cf. III.A.) suggests solvent triplet species could participate in irreversible decay. (The triplet separation in rarefied quinoline is at 0.46μ.) Unfortunately, a more intense source was not available.

To study reversible bleaching due to electronic isomerism, it is necessary that a significant change be effected with $\tau_R \ll \tau_r$. The need for crossing accuracy of the probe and the

APPENDIX

irradiation beams was mitigated, since the diffusion time between the two regions was shorter than τ_r. A high-pressure mercury lamp was used; 0.40 watt or a photon flux of 6.3×10^{17} $\sec^{-1}$ was absorbed. Fig. 3 shows the room-temperature absorption of KQS-quinoline after a constant-intensity irradiation at $\tau_R = 0$, 1 and 4 min. An isobestic point is evident here. The inserted figure, absorption of iodine in quinoline, can account for irreversible growth at 0.38μ (stage 3.a.). For $\tau_R = 1$ min a total bleaching of 50% was achieved, yet reversibility was > 90%.[10] From Fig. 3, $|A| = 0.40$ $\min^{-1}$. Since $V = 3.0$ cm^3, the bleaching rate was 1.0×10^{14} $\sec^{-1}$. Hence, $\eta (0.38\mu) = 6.3 \times 10^3$ in agreement with the low-intensity case, 5.8×10^3 (cf. Table 3). The latter value is low because irreversible bleaching was larger. The present case, corrected for the time (15 sec) taken to record the peak of the fundamental, yields $\eta (0.38\mu) = 6.6 \times 10^3$. The total bleaching per joule absorbed at 0.38μ is the same for the low and high intensity cases, (1.6 ± 0.2) $\%j^{-1}$. In spite of a scale-up factor of 10^3 in power absorbed, there is no evidence of saturation.

The results suggest additions to Model I pertinent to reversible photo-bleaching. In the scheme shown, RI and $(RI)_g$ are the trans and cis isomers, concentration n_1 and n_g, absorbing at 1.02μ and 0.90μ in KQS-quinoline, respectively. With broad-band uv, both species generate their respective $(RI)^*$, concentration n_r, causing a general reduction at the fundamental. However,
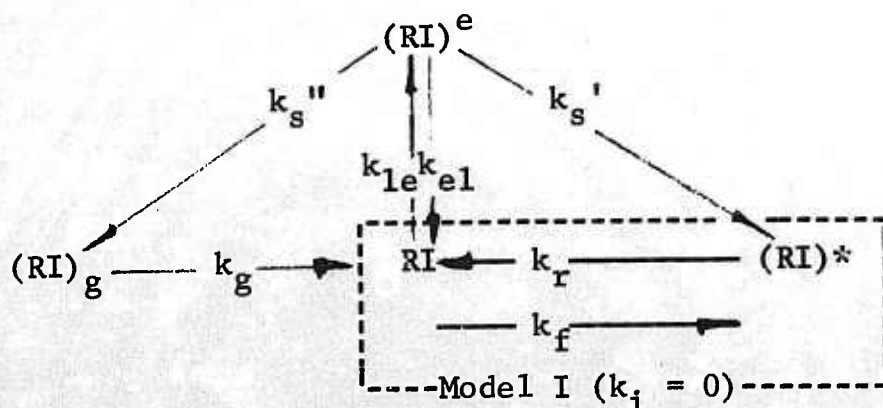
only the limiting paths to, and away from, RI are pertinent. The imbalance in the two components of the fundamental reflects geometric conversion. Pertinent to reversible bleaching, note that

$$k_{1e} \gg k_f \tag{14}$$

and

$$\tau_R < k_r^{-1} < k_g^{-1} , \tag{15}$$

i.e., recovery from electronic is faster than geometric isomerism (cf. below). At the excited level, $(RI)_e$, concentration n_e, relaxation to the ground state is overwhelming and electronic conversion is faster than geometric (cf. below),

$$k_{el} \gg k_{s'} > k_{s''} . \tag{16}$$

From the inequalities and because n_e reaches steady state $(\bar{n}_e)$ within $\Delta t \ll \tau_R$, the pertinent rates are

$$\text{(a)} \quad \dot{n}_1 = - (k_{s'} + k_{s''}) \, \bar{n}_e$$

$$\text{(b)} \quad \dot{n}_r = k_{s'} \, \bar{n}_e , \tag{17}$$

$$\text{(c)} \quad \dot{n}_g = k_{s''} \, \bar{n}_e ,$$

and

$$\frac{\bar{n}_e}{n_1} = \frac{k_{1e}}{k_{el}} \ll 1 . \tag{18}$$

The rates add up to zero in reversible bleaching. Equations (17a) and (18) account for an apparent zero-order bleaching of

the fundamental with a rate proportional to the photon flux. Recovery is a superposition of two processes: $k_{s'} \bar{n}_e \tau_R \exp(-k_r t)$ and $k_{s''} \bar{n}_e \tau_R \exp(-k_g t)$. The number of photons absorbed is $k_{1e} n_1 \tau_R$. It follows from equations (17a) and (18) that

$$\eta = \frac{k_{e1}}{k_{s'} + k_{s''}} \qquad (19)$$

and

$$\dot{n}_1 = -\frac{k_{1e}}{\eta} n_1 . \qquad (20)$$

Thus, the fractional bleaching rate and η yields k_{1e}. A separate estimate for k_{1e} is given by ρB, the induced absorption rate. The Einstein B-coefficient was derived experimentally from the absorption curve (Lorentzian distribution). The energy distribution (triangular) was centered at the peak. Fair agreement is seen between the last two columns in Table 3. The constancy of the B-coefficient may be inferred from k_{1e}, there being a photon flux density one order of magnitude higher at 0.46μ than at 0.38μ (cf. footnote to Table 3).

Room temperature recovery from a more intensive photo bleaching, 30% at $\tau_R = 6$ sec but completely reversible, is shown in Fig. 4. Two processes are seen which lead to the assignment of $\tau_r = 2.6$ min for electronic, in good agreement with thermal bleaching, and $\tau_g = 460$ min for geometric isomerism. From the amplitudes, $k_{s'}/k_{s''} = 3.4$. It follows from equation (19) that, $k_{s''} = 3.4 \times 10^{-5} k_{e1}$. Since internal conversion between higher excited states is very fast, $k_{e1} \approx k_{21} \approx 10^{11}$ sec^{-1}.[11]

In summary, for KQS-quinoline bleached at 0.38μ, at room temperature, the pertinent rate parameters are $B = 8.2 \times 10^{19}$ cm^3 erg sec^{-2}; $k_{e1} \approx 10^{11}$ sec^{-1}; $k_{s'} \approx 1.2 \times 10^7$ sec^{-1}; $k_{s''} \approx 3.4 \times 10^6$ sec^{-1}; $k_{2r} < 10^5$ sec^{-1}; $k_r = 4.4 \times 10^{-3}$ sec^{-1}; and $k_g = 2.5 \times 10^{-5}$ sec^{-1}. From $k_{s'}$ and k_{2r}, the higher excited state is two

orders of magnitude more favorable to intersystem crossing than the first excited singlet. Such is not usually the case because of efficient internal conversion.[12]

IV. CONCLUSIONS AND COMMENTS

The equilibrium, kinetic and steady-state behaviors of polymethine dye solutions were described by a three-state chain reaction involving free radicals: initiation, propagation and termination. The dark-reaction with iodine evidenced chain propagation. With oxygen the reaction was much slower, the reactive species (dye) being the triplet. The latter, as an intermediate to thermal dissociation, is characterized by $\tau_i = 10^{10}$ min at room temperature in the dark. Other k_i-paths were examined under the same conditions. Thus, $\tau_i = 10^4$ min in the presence of oxygen alone. With oxygen and moisture, $\tau_i = 8$ min and the observed rate was probably limited by transfer through the interface. Water is believed to act as a catalyst under the conditions provided, because formation of the intermediate is characterized by $\tau_f = 50$ min. Also pertinent is the sequence of solvent stability which is in the order of the separation of their first triplet with the respective ground state.

At room temperature, intersystem (nonradiative) crossing from the first triplet to the ground state is $\tau_r = 3$ min by thermal bleaching and $\tau_r = 2.6$ min by photobleaching. The specific rate for the reverse process, k_f, obtained from these values may be taken as a gauge of the discrepancy, Δk_f, in the thermal method. It can be shown that,

$$|\Delta k_f| = \frac{K}{K + I} \cdot \frac{\Delta H}{RT} \cdot \frac{|\Delta T|}{T} \lambda , \tag{21}$$

where λ is the specific rate (Newton's law) for the heating of the cell assembly. The pertinent data are: $T = 300°K$, $K = 0.074$, $\Delta H = 6800$ cal mole^{-1}, $\lambda = 0.32$ min^{-1} and $|\Delta k_f| = 0.0027$ min^{-1}.

It follows that the discrepancy corresponds to only one percent error in temperature.

A low-lying triplet contributes to the temperature dependence of the absorption coefficient, α, of the fundamental.[13] The equation of state from the model is

$$\frac{K + 1}{K} \, \alpha = \frac{\Delta H}{RT} + \text{const.,}^{[14]} \tag{22}$$

where K is temperature-dependent but not ΔH. It is desirable for repetitive Q-spoiling that

$$E_s \gg E_t \leq RT^*, \tag{23}$$

where E_s and E_t are the separations from the ground state of the first excited singlet and the lowest triplet, respectively, and T^* is the steady-state temperature for a given pulse repetition rate. Population of the triplet by either intersystem crossing is apt to be inefficient.

Due to a low-lying triplet, the long wavelength limit for Q-spoiling solutions at $\sim 300^\circ K$, is not far above 1μ. As longer chains are employed to push the fundamental past 1μ, ϵ falls rapidly. The absorption spectrum becomes flat due to various isomerizations and the solution becomes more reactive.[15] The net reaction in Model I is characterized by

$$k_I = \frac{K}{1 + K} \, k_i \, . \tag{24}$$

A comparison of k_I, benzyl iodide $(36^\circ C)^{[5]}$ vs. the polymethine chains gives 1:10:400, for benzyliodide-hexachlorobutadiene: KQS-quinoline: EQS-chlorobenzene.

Electronic and geometric conversions by photo excitation were more favorable at the higher states. Hence, crossing rates

increased with excitation faster than internal conversion. The considerable electronic isomerism effected leaves no doubt that intersystem crossing was favored at the higher state. In geometric conversion, two cases of cis-trans isomerism are possible: occurrence at a high singlet or triplet. The latter implies a low frequency factor. Since $k_{s"} = 3.4 \times 10^6$ sec^{-1}, crossing from the excited singlet is favored. Thus, the high singlet (0.38μ) was the source of branching for the two cases of isomerism, with electronic better than three times favored over geometric. However, in recovery (geometric case), $k_g = 2.5 \times 10^{-5}$ sec^{-1}, which may mean either a low frequency factor coupled with a low activation or a high frequency factor with a high activation.

Isomerization by photo excitation is influenced by the solvent. It appears necessary that the solvent absorb in the region matching the excitation of the higher states where significant branching occurs. Therefore, excited states of both solvent and solute species, or dye-solvent complex, are involved. This would provide a basis for the prevalence of irreversible bleaching in the weak-intensity case where $k_i \tau_R \approx 1$ and for the solvent-stability sequence. A modest coupling strength in the complex is in line with the observation that the balance of cis-trans isomers is dependent on the solvent and persists through moderate changes in temperature. Assuming a ratio of statistical weights close to unity for the geometric species $(RI)_g$ and RI, the observed distribution suggests an enthalpy difference of $\sim 10^2$ cal mole^{-1}, which also explains the insensitive variation of the distribution with temperature.

From these results, it is seen that the leakage from the flashlamp rather than the laser beam (1μ) is more pertinent to the steady-state performance of the Q-spoiling solution. More than 10^5 laser pulses were generated at 10 sec^{-1} before double pulsing occurred in solutions with a very low rate k_i-path.[16] Breakdown occurs at the glass-solution interface, a black smudge

APPENDIX

~ 1 mm diameter, probably caused by an inhomogeneous power density across the beam. Since a copious deposit forms before a significant decline in optical density, dye decomposition is secondary and the case is most likely solvent degradation through a chain reaction.

APPENDIX

Table 1

Summary of Constants for Thermal Bleaching
(Energy unit: cal.)

	KQS in Quinoline 40°-180°C	EQS in Chlorobenzene 35°-124°C
K	6830 exp (-6,800/RT)	4620 exp (-6,900/RT)
k_f, sec^{-1}	55 exp (-7,400/RT)	210 exp (-6,800/RT)
k_i, sec^{-1}	1.55×10^{12} exp (-32,900/RT)	2.08×10^{14} exp (-32,100/RT)

Table 2

Reversible Fraction of Total Thermal Bleaching

| Soak temp., °C	Recovery: KQS-Quinoline			Recovery: EQS-Chlorobenzene		
	Δt, min	Predicted %	Obs. %	Δt, min	Predicted %	Obs. %
80(a)	200	100	98	1000	96	94
130(b)	1000	83	84	300	0	--

(a) KQS-quinoline: $K = 0.43$ and $k_i = 4.6 \times 10^{-7}$ min^{-1}.
  EQS-chlorobenzene: $K = 0.24$ and $k_i = 1.7 \times 10^{-4}$ min^{-1}.

(b) KQS-quinoline: $K = 1.37$ and $k_i = 1.3 \times 10^{-4}$ min^{-1}.
 EQS-chlorobenzene: $K = 0.82$ and $k_i = 4.8 \times 10^{-2}$ min^{-1}.

Table 3

Bleaching of KQS Solutions

Solvent[a] $\alpha(\lambda)$, cm^{-1}	λ, μ	$-10^6 \cdot A$, sec^{-1}	D_o	F[b]	$10^{-5} \cdot \eta(\lambda)$	k_{1e}, sec^{-1}	ρB, sec^{-1}
I : 0.06	0.464	3.13	1.353	0.38	1.1	0.26	0.34
0.43	0.380	7.42	1.362	0.42	0.058	0.032	0.039
II: 0.02	0.467	4.43	1.277	0.65	1.3	0.45	0.83
0.05	0.384	2.00	1.255	0.41	0.21	0.033	0.045

(a) I = quinoline, II = chlorobenzene and $I = I_o \exp(-\alpha \ell)$

(b) Incident photon flux density: $I_o (0.38\mu) = 1.5 \times 10^{15}$ sec^{-1} and $I_o (0.46\mu) = 1.4 \times 10^{16}$ sec^{-1}.

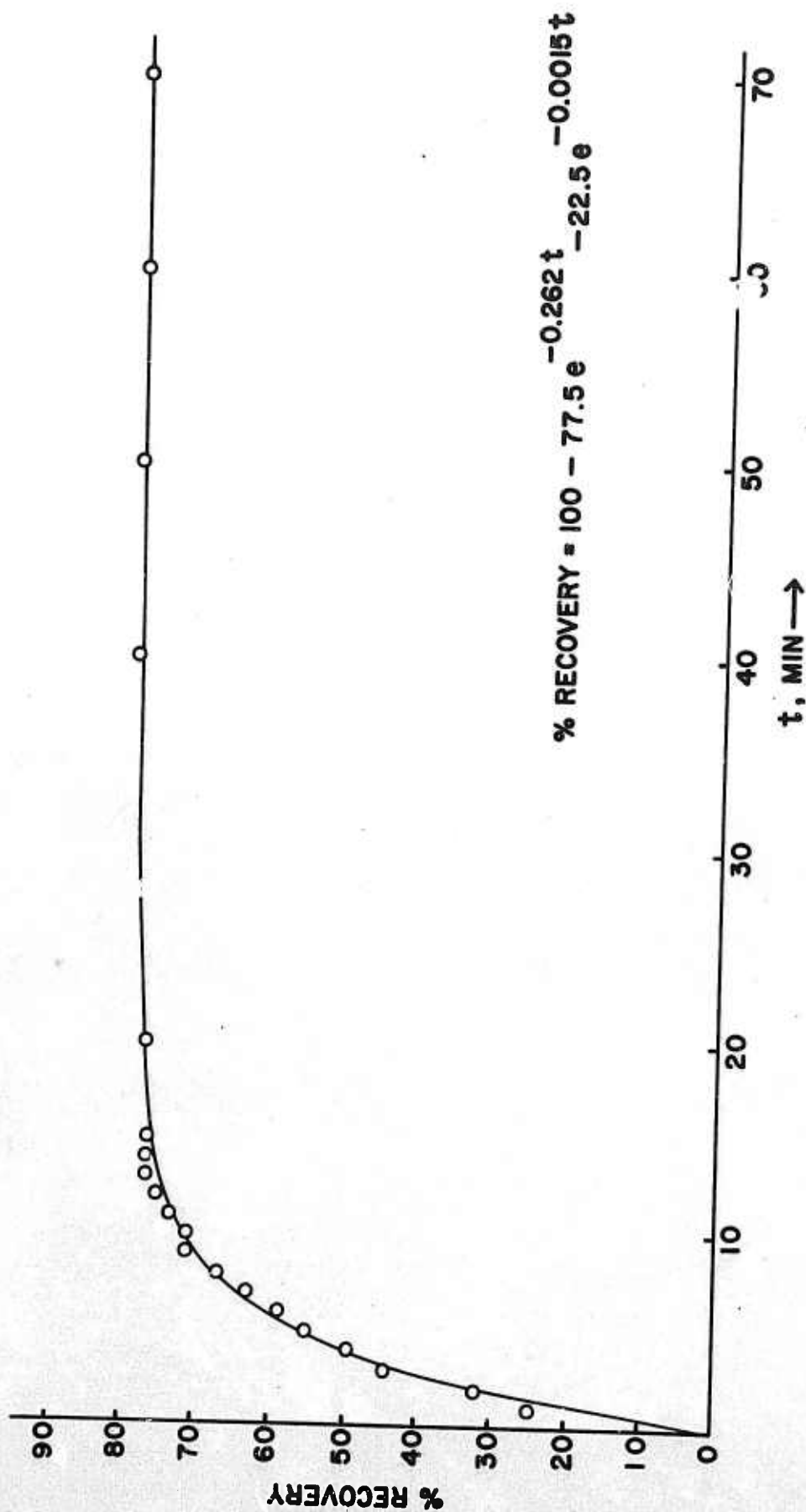$$\% \text{ RECOVERY} = 100 - 77.5\,e^{-0.262\,t} - 22.5\,e^{-0.0015\,t}$$
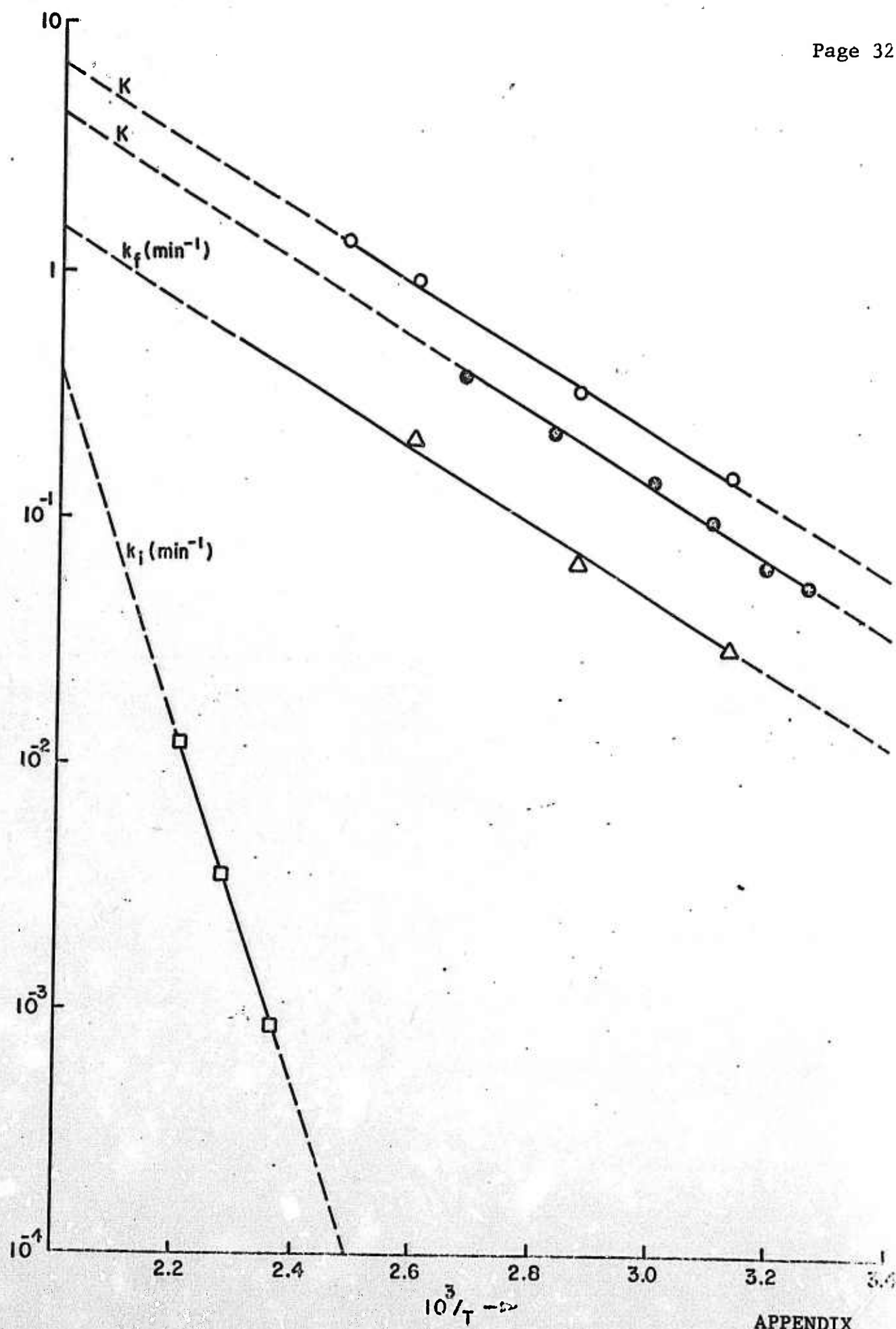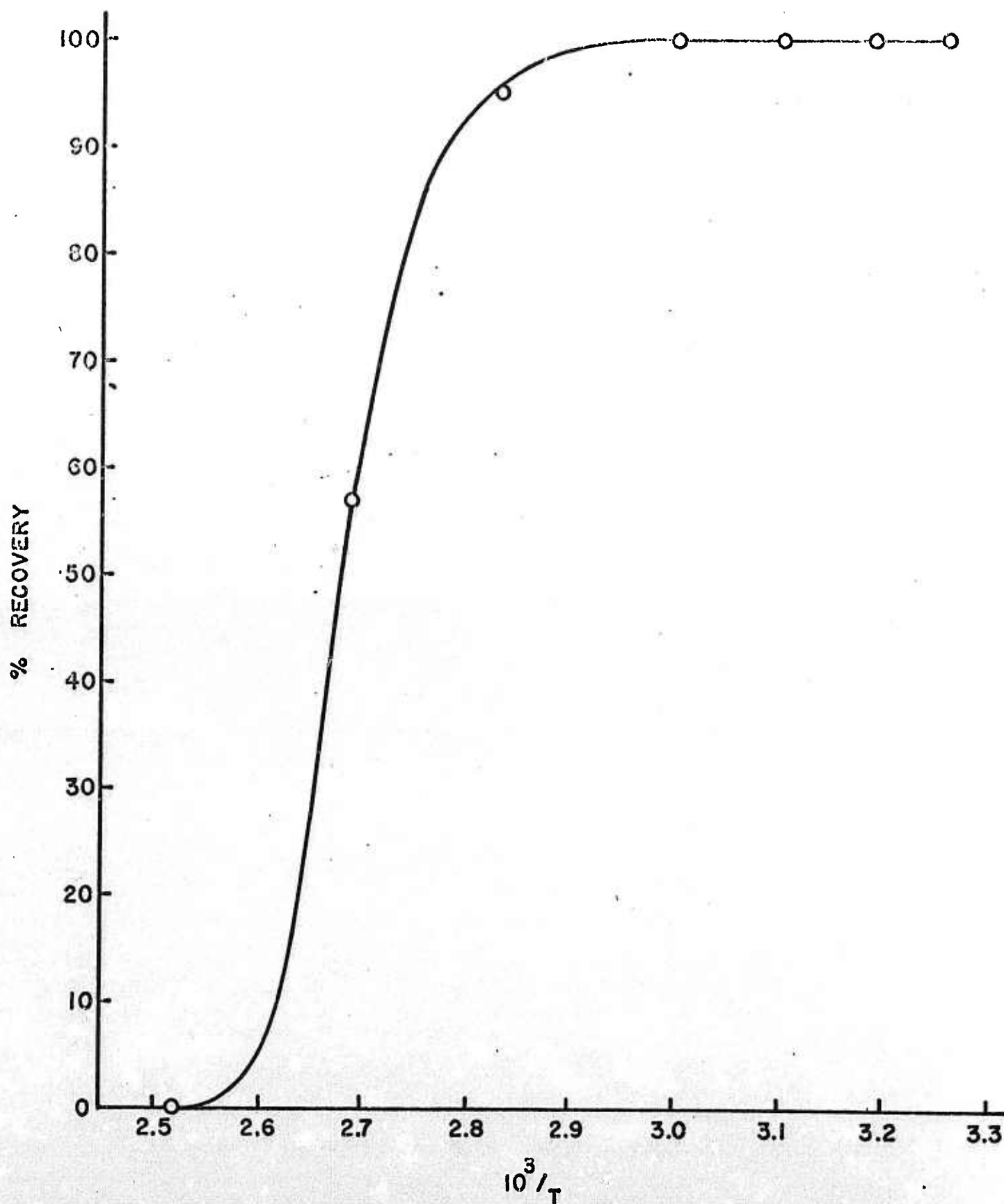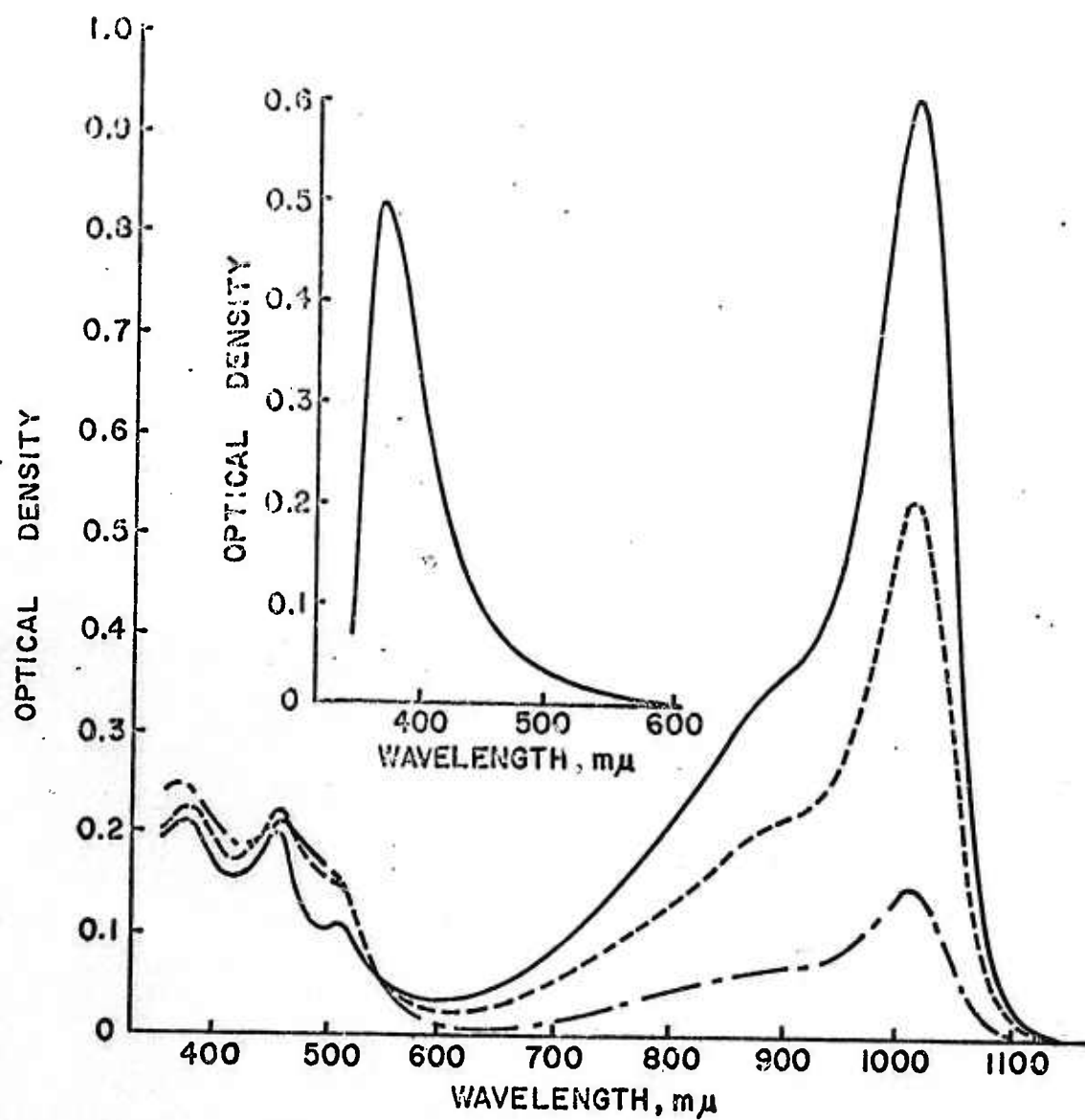
FIGURE CAPTIONS

Fig. 1   Equilibrium constant, K, and specific rates, k, vs.
T^{-1}. KQS-quinoline (0, Δ, $\square$) and EQS-chlorobenzene ($\bullet$).

Fig. 2   Room-temperature recovery of EQS-chlorobenzene follow-
ing 1200 min exposures at various temperatures. The
curve is calculated from K and k_i. Circles stand for
observations.

Fig. 3   Room-temperature absorption of KQS-quinoline.

—— τ_R = 0 min

---- τ_R = 1 min

— - τ_R = 4 min

Insert spectrum is the absorption of I_2-quinoline.

Fig. 4   Room-temperature recovery of the fundamental absorption
of KQS-quinoline photo bleached by irradiating at 0.38μ.

FOOTNOTES

1   B. H. Soffer, J. Appl. Phys. <u>35</u>, 2551 (1964); P. Kafalas, J. I. Masters, and E. M. Murray, op. cit., 2349 (1964).

2   B. H. Soffer and R. H. Hoskins, Nature <u>204</u>, 276 (1964). Like kryptocyanine, KQS is also a carbocyanine. The formula and preparation (literature) is given in the reference cited.

3   "Eastman Q-switch Solution 9740," a circular released by Distillation Products Industries (Oct. 1965).

4   Bleaching alludes to the fundamental absorption of species RI.

5   M. Gazith and R. M. Noyes, J. Am. Chem. Soc. <u>77</u>, 6091 (1955).

6   The effect is obtained also with kryptocyanine or EQS. With aromatic solvents, the behavior is complicated, presumably by iodine-solvent complexing.

7   A low-lying triplet, 7 kcal mole^{-1} in the present case, is not unexpected for a conjugated chain of 13-C atoms. The Chichibabin hydrocarbon, 18-C chain, has the triplet at 3 kcal mole^{-1} (cf. C. A. Hutchison, A. Kowalsky, R. C. Pastor, and G. W. Wheland, J. Chem. Phys. <u>20</u>, 1485 (1952) and references cited).

8   Intramolecular resonance stabilizes the polar form, R^+I^-. The similar charge on the ends of the polymethine chain (R) favor the trans arrangements which account for the structure at the longer-wavelength region of the fundamental absorption. See L. G. S. Brooker, p. 573, in "Recent Progress in the Chemistry of Natural and Synthetic Colouring Matters and Related Fields," edited by T. S. Gore, B. S. Joshi, S. V. Sunthankar, and B. D. Tilak (Academic Press, 1962).

9   An interpretation based on dissociation of higher aggregates is not compatible with the results of thermal bleaching.

10   In the low-intensity case (0.38μ, cf. Table 3), the photon absorption rate, 7.4×10^{14} sec^{-1}, is three orders lower but the total bleaching is only one order lower. The present case shows photo-dissociation (net reaction of stage 1) can be avoided; otherwise, rapid irreversible bleaching occurs (stage 2).

11   The Einstein A-coefficient (spontaneous emission) at 0.38μ, for KQS-quinoline, is only 1.1×10^9 sec^{-1}, a negligible contribution to k_{el}.

12   F. Wilkinson, Quart. Revs. XX (No. 3), 403 (1966).

13   From the data, reversible thermal bleaching at 27°C is -0.26% deg^{-1} for KQS-quinoline and -0.11% deg^{-1} for EQS-chlorobenzene. Thermal expansion of the solvent (quinoline) adds -0.08% deg^{-1}.

APPENDIX

14   From $\alpha = \sigma N$, the absorption cross-section, σ, is inde-
      pendent of T; thus, $d\ln \alpha/dT = d\ln N/dT$, where N is the
      density of absorbers.

15   See reference in footnote 8 and also, S. S. Malhotra
      and M. C. Whiting, J. Chem. Soc. 3812 (1960).

16   A Nd-YAG laser was used, 26j input and peak power $\sim$ 3 Mw
      for the pulses. Volume of the solution was 3 cm^3.

Security Classification

DOCUMENT CONTROL DATA - R&D
(Security classification of title, body of abstract and indexing annotation must be entered when the overall report is classified)

1. ORIGINATING ACTIVITY (Corporate author)	2a. REPORT SECURITY CLASSIFICATION
KORAD CORPORATION 2520 Colorado Avenue Santa Monica, California	UNCLASSIFIED
	2b. GROUP None

3. REPORT TITLE

SPECTRAL PROPERTIES OF PASSIVELY Q-SPOILED LASERS

4. DESCRIPTIVE NOTES (Type of report and inclusive dates)

SemiAnnual Technical Summary Report from 1 Apr 1967 thru 30 Sept 1967

5. AUTHOR(S) (Last name, first name, initial)

SOFFER, B H
PASTOR, R C

6. REPORT DATE	7a. TOTAL NO. OF PAGES	7b. NO. OF REFS
30 October 1967	49	--

8a. CONTRACT OR GRANT NO. Nonr-5150 (00)	9a. ORIGINATOR'S REPORT NUMBER(S)
b. PROJECT NO. ARPA Order Nr 306	
c. Project Code Nr 015-710	9b. OTHER REPORT NO(S) (Any other numbers that may be assigned this report)
d.	

10. AVAILABILITY/LIMITATION NOTICES

Reproduction in whole or in part is permitted for any purpose
of the United States Government.

11. SUPPLEMENTARY NOTES	12. SPONSORING MILITARY ACTIVITY This research is part of Project DEFENDER under the joint sponsorship of ARPA, ONR, and DOD.

13. ABSTRACT

Two new blue-violet organic dye lasers are described. Another blue-violet system, a frequency doubled near-infrared organic dye laser, is also described. The results of incorporating a bleachable absorber into the organic dye laser cavity are discussed. Further developments in the study of photobleaching of dyes used for Q-spoiling the Nd laser are reported. A preprint of an article submitted for publication, based on work supported by this contract is reproduced as an Appendix.

DD FORM 1473
1 JAN 64

14. KEY WORDS	LINK A		LINK B		LINK C	
	ROLE	WT	ROLE	WT	ROLE	WT
Lasers						
Organic Dye Lasers						
Q-Spoiling Dyes						

INSTRUCTIONS

1. **ORIGINATING ACTIVITY:** Enter the name and address of the contractor, subcontractor, grantee, Department of Defense activity or other organization (*corporate author*) issuing the report.

2a. **REPORT SECURITY CLASSIFICATION:** Enter the overall security classification of the report. Indicate whether "Restricted Data" is included. Marking is to be in accordance with appropriate security regulations.

2b. **GROUP:** Automatic downgrading is specified in DoD Directive 5200.10 and Armed Forces Industrial Manual. Enter the group number. Also, when applicable, show that optional markings have been used for Group 3 and Group 4 as authorized.

3. **REPORT TITLE:** Enter the complete report title in all capital letters. Titles in all cases should be unclassified. If a meaningful title cannot be selected without classification, show title classification in all capitals in parenthesis immediately following the title.

4. **DESCRIPTIVE NOTES:** If appropriate, enter the type of report, e.g., interim, progress, summary, annual, or final. Give the inclusive dates when a specific reporting period is covered.

5. **AUTHOR(S):** Enter the name(s) of author(s) as shown on or in the report. Enter last name, first name, middle initial. If military, show rank and branch of service. The name of the principal author is an absolute minimum requirement.

6. **REPORT DATE:** Enter the date of the report as day, month, year; or month, year. If more than one date appears on the report, use date of publication.

7a. **TOTAL NUMBER OF PAGES:** The total page count should follow normal pagination procedures, i.e., enter the number of pages containing information.

7b. **NUMBER OF REFERENCES:** Enter the total number of references cited in the report.

8a. **CONTRACT OR GRANT NUMBER:** If appropriate, enter the applicable number of the contract or grant under which the report was written.

8b, 8c, & 8d. **PROJECT NUMBER:** Enter the appropriate military department identification, such as project number, subproject number, system numbers, task number, etc.

9a. **ORIGINATOR'S REPORT NUMBER(S):** Enter the official report number by which the document will be identified and controlled by the originating activity. This number must be unique to this report.

9b. **OTHER REPORT NUMBER(S):** If the report has been assigned any other report numbers (*either by the originator or by the sponsor*), also enter this number(s).

10. **AVAILABILITY/LIMITATION NOTICES:** Enter any limitations on further dissemination of the report, other than those imposed by security classification, using standard statements such as:

  (1) "Qualified requesters may obtain copies of this report from DDC."

  (2) "Foreign announcement and dissemination of this report by DDC is not authorized."

  (3) "U. S. Government agencies may obtain copies of this report directly from DDC. Other qualified DDC users shall request through

  _____ ."

  (4) "U. S. military agencies may obtain copies of this report directly from DDC. Other qualified users shall request through

  _____ ."

  (5) "All distribution of this report is controlled. Qualified DDC users shall request through

  _____ ."

If the report has been furnished to the Office of Technical Services, Department of Commerce, for sale to the public, indicate this fact and enter the price, if known.

11. **SUPPLEMENTARY NOTES:** Use for additional explanatory notes.

12. **SPONSORING MILITARY ACTIVITY:** Enter the name of the departmental project office or laboratory sponsoring (*paying for*) the research and development. Include address.

13. **ABSTRACT:** Enter an abstract giving a brief and factual summary of the document indicative of the report, even though it may also appear elsewhere in the body of the technical report. If additional space is required, a continuation sheet shall be attached.

It is highly desirable that the abstract of classified reports be unclassified. Each paragraph of the abstract shall end with an indication of the military security classification of the information in the paragraph, represented as *(TS), (S), (C), or (U)*.

There is no limitation on the length of the abstract. However, the suggested length is from 150 to 225 words.

14. **KEY WORDS:** Key words are technically meaningful terms or short phrases that characterize a report and may be used as index entries for cataloging the report. Key words must be selected so that no security classification is required. Identifiers, such as equipment model designation, trade name, military project code name, geographic location, may be used as key words but will be followed by an indication of technical context. The assignment of links, roles, and weights is optional.